

# Performance Analysis of Free-Space Optical Communication Transceiver

Omkar Naidu V<sup>1</sup>, K.M Hemambaram<sup>2</sup>, Neerajakshi.V<sup>3</sup>, Kantaraju<sup>4</sup>

<sup>1</sup>Department of ECE, SITAMS, Chittoor, Andhra Pradesh, India

<sup>2</sup>Assistant Professor, Department of ECE, SITAMS, Chittoor, Andhra Pradesh, India

<sup>3,4</sup>Department of ECE, BIT Institute of Technology, Hindupur, Andhra Pradesh, India

## Abstract

A novel paper, in this we inspect the cooperative diversity method as a candidate solution for combating commotion -induced fading over Free-Space Optical (FSO) links. In particular, a one spread cooperative range scheme is proposed and analyzed for non-coherent FSO communications with intensity modulation and direct detection (IM/DD). The error performance is derived in semi-analytical and closed-form expressions in the presence and absence of background radiation, respectively. Results show the enhanced diversity orders that can be achieved over both Rician Channel models.

**Index Terms**—Free-space optics, spatial diversity, cooperative diversity, atmospheric turbulence.

## 1. INTRODUCTION

NEWLY, Free-Space Optical (FSO) communications attracted significant attention as a promising solution for the “last mile” problem, degrades the link performance is fading (or scintillation) that results from the variations of the index of refraction due to in homogeneities in temperature and pressure changes [2]. In order to maintain suitable performance levels over FSO links, fading-mitigation techniques for instance spatial diversity techniques must be employed. Spatial diversity involves the deployment of multiple transmit and/or receiver apertures and is generally used to combat fading and improve the link consistency. Diversity combining techniques were extensively studied in the context of radio-frequency (RF) wireless transmissions and were newly extended and tailored to FSO transmissions. In this circumstance, aperture-averaging receiver diversity [3],

spatial repetition codes [4], unipolar versions of the orthogonal space-time codes [5] and transmit laser selection [6] were proposed as FSO- tailored spatial diversity solutions. In the same way, the bit error rates of Multiple-Input-Multiple-Output (MIMO) FSO links were executed in [7] and [8].

On the other hand, in RF systems cooperative diversity techniques are becoming extra admired in situations where few number of antennas can be deployed at the mobile terminals [9], [10]. In this context, neighboring nodes can form “virtual” antenna arrays and profit from the core spatial diversity in a distributed manner. Cooperative diversity takes add of the broadcast nature of RF transmissions where a message transmitted from a cause to a destination can be neighboring overheard by nodes. If these nodes are willing to Cooperate with the source; they retransmit information about the same message to the destination thus enhancing the quality of signal reception. Despite the extensive research in RF wireless cooperation, to the authors’ best knowledge, this technique was never considered before in the context of FSO communications.

In this paper, we investigate for the first time the value of cooperative diversity as a means of combating fading in FSO links. In particular, we consider a decode-and-forward approach with one relay over FSO links with intensity modulation and direct detection (IM/DD). Pulse-position modulation, or PPM, is a powerful and widely used technique for transmitting information over an optical direct-detection channel.

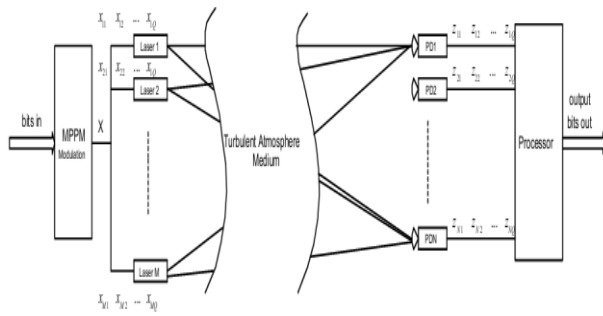


Figure 1.1: System block diagram of free space optical communications

PPM is a modulation technique that uses pulses that are of uniform amplitude and width but displaced in time by an amount depending on the data to be transmitted. It is also sometimes known as pulse-phase modulation. It has the advantage of requiring constant transmitter power since the pulses are of constant amplitude and duration. PPM also has the advantage of good noise immunity since all the receiver needs to do is detect the presence of a pulse at the correct time; the duration and amplitude of the pulse are not important.

The main reason that discourages the investigation of cooperation in FSO systems resides in the non-broadcast nature of optical transmissions. In FSO, the source can not broadcast an information message to the destination and to a distant relay simultaneously. Consequently, an additional transmit power must be completely dedicated for delivering the message to the relay. None of this power will reach the destination implying an additional power penalty (as compared to RF wireless cooperation). Though, this work shows that the cooperative diversity can be of use in enhancing the performance of FSO links since the add in diversity can compensate for this power penalty.

On the other hand, the factors encouraging the implementation of the cooperative diversity technique are as follows. (1): The solution is cost-effective (compared to MIMO-FSO) since it does not require adding more apertures to the transmitter and/or receiver. (2): It is well known that channel correlation degrades the performance of MIMO systems whether in FSO or RF scenarios. However, MIMO-FSO channels are more likely to be correlated. In fact, in RF systems the signal reaches the receiver by a large number of paths implying that a small separation between the antennas can ensure a channel independence. Further, FSO links are a lot more directive thus depiction the path gains between the transmit and receive elements more dependent; for example, the presence of a small cloud between the transmitter and

receiver can make large fades on all source-detector pairs simultaneously [4].

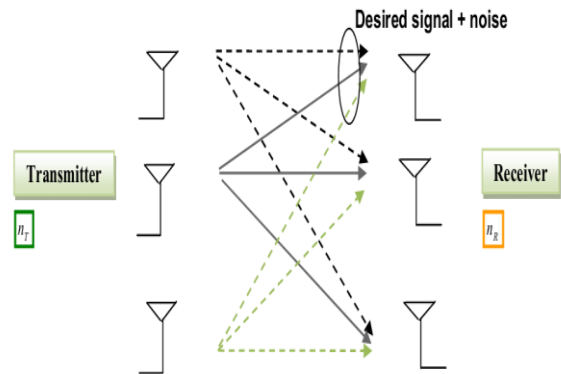


Figure 1.2: Multiple-Input-Multiple-Output (MIMO) system

As a result, the high performance gains promised by MIMO-FSO solutions under the principle of channel independence [4]–[6] might not be achieved in practice. Thus, as stated in [4] “An alternative operation in such environments must be calculated”. In this context, assistance can compose a good candidate alternative. In fact, given the large distances (in the order of kilometers) between the source-destination, source-relay and relay-destination, the assumption of independence is more applicable compared to the case of co-located arrays

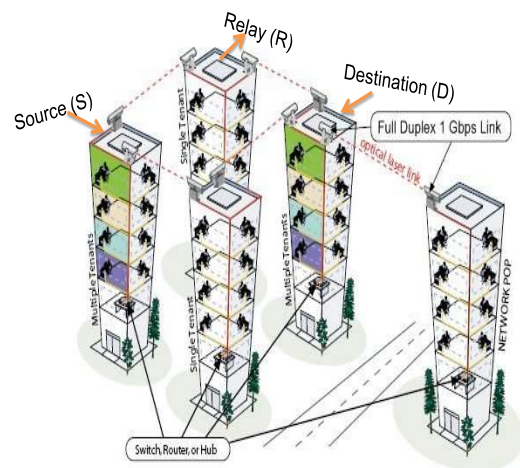


Fig. 1.3 An example of a mesh FSO network. Cooperation is proposed among the transceivers on buildings (1), (2) and (3) where the transceivers on building 2 can help in transmitting an information message from (1) to (3). Note how, given the non-

broadcast nature of FSO transmissions, one couple of FSO transceiver units is dedicated for each link.

(3): Unlike RF systems, extending the MIMO techniques to FSO systems imposes a compromise on the choice of the sources. Sources have to be low adequate to couple more power from the transmitter to the recipient and they must be wide sufficient to illuminate all detectors simultaneously.

As a result, the wider spacing of detectors (necessary for channel independence) results in an enlarged transmit power. In this circumstance, taking advantage of the spatial diversity in a distributed manner by deploying the projected cooperative scheme permits to overcome this limitation and can constitute a good practical alternative to MIMO-FSO systems

## II.STRUCTURE AND SYSTEM MODEL AT TRANSMITTER

Consider the example of a FSO Metropolitan Area Network as shown in Fig. 1. Consider three neighboring buildings (1), (2) and (3) and suppose that a FSO connection is available between each building and its two neighboring buildings. In FSO networks, each one of these connections is established via FSO-based wireless units each consisting of an optical transceiver with a transmitter and a receiver to offer full-duplex capability. Given the high directivity and non-broadcast life of FSO transmissions, one part transceiver is entirely keen for the communication with each neighboring building. We assume that the transceivers on building (2) are available for cooperation to improve the communication reliability between buildings (1) and (3). By cruelty of notations, buildings (1), (2) and (3) will be denoted by source (S), relay (R) and destination (D), respectively.

The cooperation strategy is show in Fig. 2. It is value noting that the transceivers at (R) are not deployed with the objective of assisting (S). In fact, these transceivers are deployed for (R) to communicate with (S) and (D); if (R) is willing to share its existing resources (and (R) has no information to transmit), then it can act as a relay for assisting (S) in its communication with (D). The cooperation strategy is as follows: a sequence of symbols is first transmitted to the relay. At a second time, (R) transmits the decoded symbols to (D) while (S) transmits the same sign progression simultaneously to (D).

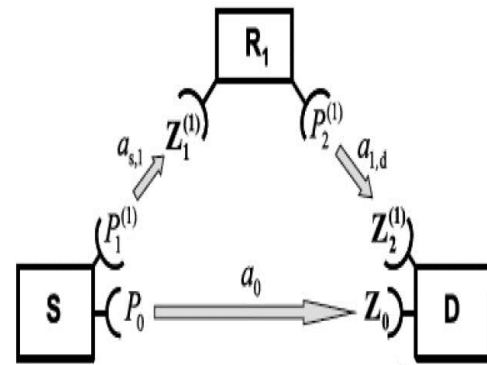


Figure 2.1: cooperative scheme

Since three transmissions are involved in each cooperation cycle, then the transmitted power from transceivers TRxS,1, TRxS,2 and TRxR,2 must be divided by 3, Denote by  $a_0$ ,  $a_1$  and  $a_2$  the random path gains between S-D, S-R and R-D, respectively. The system models in our work adopt Rayleigh, lognormal Rician turbulence-induced fading channels[4].

The probability density function (pdf) for Rayleigh channels is:

$$f_A(a) = 2ae^{-a^2} \tag{1}$$

In the lognormal model, the probability density function (pdf) of the path gain ( $a > 0$ ) is given by:

$$f_A(a) = \frac{1}{\sqrt{2\pi}\sigma_a} \exp\left(-\frac{(\ln a - \mu)^2}{2\sigma^2}\right) \tag{2}$$

where the parameters  $\mu$  and  $\sigma$  satisfy the relation  $\mu = -\sigma^2$  so that the path intensity is unity:  $E[A] = E[A^2] = 1$ . The degree of fading is measured by the scintillation index defined by: S.I. =  $e^{4\sigma^2} - 1$ . Typical values of S.I. range between 0.4 and 1. In the Rician model, the pdf of the path gain ( $a > 0$ ) is:  $f_A(a) = 2ae^{-a^2}$ . Consider  $Q$ -ary pulse position modulation (PPM) with IM/DD links where the receiver corresponds to a photoelectrons counter. Consider first the link S-D and denote by  $Z^{(0)} = [Z_1^{(0)}, Z_2^{(0)} \dots Z_Q^{(0)}]$  the  $Q$ -dimensional vector whose  $q$ -th component  $Z_q^{(0)}$  corresponds to the number of photoelectron counts in the  $q$ -th slot. Denote the transmitted symbol by  $s \in \{1, \dots, Q\}$ . The decision variable  $Z_s^{(0)}$  can be modeled as a Poisson random variable (r.v.) with parameter  $\frac{a_0^2 \lambda_s}{3} + \lambda_n$  while  $Z_q^{(0)}$  (with  $q \neq s$ ) can be modeled as a Poisson r.v. with parameter  $\lambda_n$  [4]:

$$Pr(Z_q^{(0)} = k) = \begin{cases} \frac{e^{-\left(\frac{a_0^2 \lambda_s}{3} + \lambda_n\right)} \left(\frac{a_0^2 \lambda_n}{3} + \lambda_n\right)^k}{k!}, & q = s; \\ \frac{e^{-\lambda_n} \lambda_n^k}{k!}, & q \neq s; \end{cases} \quad (3)$$

where  $\lambda_s$  (resp.  $\lambda_n$ ) corresponds to the average number of photoelectrons per slot due to the light signal (resp. background radiation and “dark currents”)

$$\lambda_s = \eta \frac{P_r T_s / Q}{hf} = \eta \frac{E_s}{hf} \quad (4)$$

where  $\eta$  is the detector’s quantum efficiency assumed to be equal to 1 in what follows,  $h = 6.6 \times 10^{-34}$  is Planck’s constant and  $f$  is the optical center frequency taken to be  $1.94 \times 10^{14}$  Hz (corresponding to a wavelength of 1550 nm).  $T_s$  stands for the symbol duration,  $P_r$  stands for the optical power that is incident on the receiver and  $P_b$  corresponds to the incident background power. Finally,  $E_s = P_r T_s / Q$  corresponds to the received optical energy per symbol corresponding to the direct link S-D. Readers can refer to [4] for more details on the system model. In the same way, we denote the decision vector corresponding to the S-R link by  $Z^{(1)} = [Z_1^{(1)}, Z_2^{(1)} \dots Z_Q^{(1)}]$  where the

$$E[Z_q^{(1)}] = \begin{cases} \beta_1 \frac{a_1^2 \lambda_s}{3} + \lambda_n, & q = s; \\ \lambda_n, & q \neq s; \end{cases} \quad (5)$$

where  $\beta_1$  is a gain factor that follows from the fact that (S) might be closer to (R) than it is to (D). In other words, the received optical energy at (R) corresponding to  $E_s$  (that corresponds to the S-D link) is  $\beta_1 E_s$ . Performing a typical link budget analysis [4] shows that  $\beta_1 = \left(\frac{d_{SD}}{d_{SR}}\right)^2$  where  $d_{SD}$  and  $d_{SR}$  stand for the distances from (S) to (D) and (S) to (R) respectively. The maximum-likelihood (ML) decision rule at (R) is given by:  $\hat{S} = \arg \max_{q=1, \dots, Q} Z_q^{(1)}$ . The relay transmits the symbol  $\hat{S}$  along the link R-D implying that the corresponding decision vector can be written as  $Z^{(2)} = [Z_1^{(2)}, Z_2^{(2)} \dots Z_Q^{(2)}]$  where  $Z_Q^{(2)}$  is a Poisson r.v. with:

$$E[Z_q^{(2)}] = \begin{cases} \beta_2 \frac{a_2^2 \lambda_s}{3} + \lambda_n, & q = \hat{S}; \\ \lambda_n, & q \neq \hat{S}; \end{cases} \quad (6)$$

where  $\beta_2 = \left(\frac{d_{SD}}{d_{RD}}\right)^2$  with  $d_{RD}$  corresponding to the distance between (R) and (D). Finally, note that the normalization of  $\lambda_s$  by 3 in equations (4), (5) and (6) ensures that the total transmit power is the same as in non-cooperative systems.

### III. FLOW AT RECEIVER

As in all cooperative schemes, decoding will be based on the assumption:  $P_e \triangleq \Pr(\hat{S} \neq S) \ll 1$ . This is necessary since these schemes result in performance gains only for large values of  $E_s$ .

#### A. Detection without Background Radiation

In the absence of background radiation,  $Z^{(0)}$  and  $Z^{(2)}$  contain at least  $Q-1$  empty slots each. In this case, the detection procedure at (D) is as follows. If one component of  $Z^{(0)}$  is different from zero, this will imply that the symbol  $s$  was transmitted in the corresponding slot since in the absence of setting radiation the only source of this nonzero count is the presence of a light signal in this slot. On the other hand, if all components of  $Z^{(0)}$  are equal to zero, then the decision will be based on  $Z^{(2)}$ . If one component of  $Z^{(2)}$  is diverse from zero, then with probability  $1 - P_e$  this component corresponds to  $s$  and with probability  $P_e$  this component corresponds to an erroneous slot. Since  $1 - P_e$  is assumed to be greater than  $P_e$  (since  $P_e \ll 1$ ), then the best strategy is to decide in favor of the nonempty slot of  $Z^{(2)}$ . Finally, if all components of  $Z^{(0)}$  and  $Z^{(2)}$  are equal to zero, then (D) decides randomly in favor of one of the  $Q$  slots. To summarize, (D) decides in favor of  $\hat{S}$  according to the following strategy:

$$\hat{S} = \begin{cases} \arg q [Z_q^{(0)} \neq 0], & Z^{(0)} \neq \mathbf{0}_Q; \\ \arg q [Z_q^{(2)} \neq 0], & Z^{(0)} = \mathbf{0}_Q, Z^{(2)} \neq \mathbf{0}_Q; \\ \text{rand}(1, \dots, Q), & Z^{(0)} = Z^{(2)} = \mathbf{0}_Q; \end{cases} \quad (7)$$

Where  $\mathbf{0}_Q$  corresponds to the  $Q$ -dimensional all-zero vector while the function  $\text{rand}(1, \dots, Q)$  corresponds to choosing randomly one integer in the set  $\{1, \dots, Q\}$ .

#### B. Detection in the Presence of Background Radiation

In this case, the background radiation results in nonzero counts even in empty slots necessitating a more complicated detection procedure. The optimal ML detection procedure must take into consideration that  $\hat{s}$  might be different from  $s$ . Note that  $\hat{S} = s$  with probability  $1 - P_e$  while  $\hat{S}$  can correspond to a certain slot that is different from  $s$  with probability  $P_e / (Q-1)$ . In this case, eliminating all common terms in the log-likelihood function, it can be proven that the ML decision rule is given by:

$$(\hat{S}, \hat{S}) = \text{arg} g_{q,q' \in \{1..Q\}} \max \left[ Z_q^{(0)} \ln \left( 1 + \frac{a_0^2 \lambda_s}{3\lambda_n} \right) + Z_q^{(2)} \ln \left( 1 + \beta_2 \frac{a_2^2 \lambda_s}{3\lambda_n} \right) \right] + \begin{cases} \ln(1 - P_e), & q = q'; \\ \ln \left( \frac{P_e}{Q-1} \right), & q \neq q'; \end{cases} \quad (8)$$

Even though optimal, the above decoder is not feasible for practical implementation since it requires the knowledge of  $P_e$  which is not available. On the other hand, given that  $P_e \ll 1$ , then we can build a simpler decoder that is based on the assumption that the decision made at the relay is correct ( $\hat{S} = S$ ). In this case, the decision rule given in eq. (6) simplifies to:

$$\tilde{S} = \text{arg} g_{q \in \{1..Q\}} \max \left[ Z_q^{(0)} \ln \left( 1 + \frac{a_0^2 \lambda_s}{3\lambda_n} \right) + Z_q^{(2)} \ln \left( 1 + \beta_2 \frac{a_2^2 \lambda_s}{3\lambda_n} \right) \right] \quad (9)$$

Equation (9) corresponds to evaluating weighted sums of the photoelectron counts. An even simpler decision rule adopts equal weights and is given by:

$$\tilde{S} = \text{arg} g_{q \in \{1..Q\}} \max [Z_q^{(0)} + Z_q^{(2)}] \quad (10)$$

In this paper, we adopt the equal-gain combiner (EGC) described in eq. (8) for the following reasons. (i) Simulations showed that the performance levels achieved by the decoders given in equations (6), (7) and (8) are very close to each other. In fact, for practical values of  $ES$ , the decoders in equations (6) and (7) are extremely close to each other (which is justified since  $P_e \ll 1$ ) and their performance gain with respect to EGC is negligible. (ii) The implementation of EGC is much simpler since it does not require any form of training for acquiring the values of the channel gains as well as  $\lambda_s$  and  $\lambda_n$ .

Finally, equations (5) and (8) show that the proposed cooperation strategy can be implemented without requiring any channel state information neither at the transmitter nor at the receiver sides.

#### IV. RICIAN CHANNEL

When we transmit any data without any coding by AWGN, Rician or Rician fading channel then it needs very high SNR to receive it and has very bad error performance. But in satellite transmission rician channel is generally considered for line of sight (LOS) communication. For bit error rate 10<sup>-5</sup> the bitrates according to SNR. In transmission we generally use Rician fading channel. Now we will make analysis of joint performance in Rician channel. In figure 6, 7, 8 we get better performance of Huffman-Convolutional, Huffman-Reed Solomon, Huffman BCH coding in Rician channel which are better than transmission of uncoded data in AWGN channel

It is well known that a communication system consists of two essential functional modules, the source codec and channel codec. These two modules are essentially concerned with data compression and transmission. In data compression, we strive to remove all the redundancy from the data to achieve a compressed representation of the data most close to the entropy of the source.

$$R(t, k) = \sqrt{\frac{2}{M}} \sum_{n=1}^M A_k(n) (\cos \beta_n + j \sin \beta_n) \cos(2\pi f_n t + \theta_n) \quad (11)$$

On the other hand, in data transmission, we intentionally add redundancy into data in a controlled fashion to combat channel noise. Therefore, joint source-channel coding may improve end-to-end system performance. More importantly, the optimum performance of joint source channel coding could be applied to practical contexts such as voice, image and video communication systems. It will be possible to transmit data with sufficient bitrate with lower error performance and minimum power by optimum performance of joint source channel coding.

#### V. PERFORMANCE ANALYSIS

Because of the symmetry of the PPM constellation, we evaluate the error performance of the proposed scheme assuming that the symbol  $s = 1$  was transmitted. The symbol-error probability (SEP) conditioned on the channel state  $A \triangleq [a_0, a_1, a_2]$  is:

$$P_{e|A} = Pr(Z_1^{(0)} > 0) p_0 + Pr(Z_1^{(0)} = 0) [Pr(Z_s^{(2)} = 0) p_1 + Pr(Z_s^{(2)} > 0) ((1 - P_e) p_2 + p_e p_3)] \quad (12)$$

where  $p_0 = 0$  since no error is made when there is at least one photoelectron in the first slot.  $p_1 = \frac{Q-1}{Q}$  since when  $Z^{(0)} = Z^{(2)} = 0_Q$  a random decision is made among the  $Q$  slots.  $p_2 = 0$  since when a correct decision is made at (R) ( $\hat{S}=1$  with probability  $1 - P_e$ ) and  $Z_1^{(2)} > 0$  completed, a correct decision will be made at (D) as well. Finally,  $p_3 = 1$  since when (R) decides erroneously in errand of a symbol  $\hat{S} \neq 1$  (with probability  $P_e$ ) and the count in the corresponding  $\hat{S}$ -th slot of  $Z^{(2)}$  is nonzero, then (D) will too decide in favor of  $\hat{S}$  resulting in a error.

$$P_e = \int_0^\infty \int_0^\infty \int_0^\infty P_{e|A} f_A(a_0) f_A(a_1) f_A(a_2) da_0 da_1 da_2 \quad (13)$$

where because of the form of  $P_{e|A}$ , the above integral can be split into three separate integrals. For lognormal fading, eq. (13) does not admit a closed-form solution and it can be written as:

$$P_e = \frac{Q-1}{Q} [P_{e,0} P_{e,2} + P_{e,0} P_{e,1} - P_{e,0} P_{e,1} P_{e,2}] \quad (14)$$

where  $P_{e,0} \triangleq \text{Fr}(\lambda s^3, 0, \sigma)$ ,  $P_{e,1} \triangleq \text{Fr}(\beta^1 \lambda s^3, 0, \sigma)$  and  $P_{e,2} \triangleq \text{Fr}(\beta^2 \lambda s^3, 0, \sigma)$  where  $\text{Fr}(a, 0, b)$  is the lognormal density frustration function defined in [11] as:

$$\text{Fr}(a, 0, b) = \int_0^\infty \frac{1}{\sqrt{2\pi b^2 x}} \exp(-ax^2) \exp\left[-\frac{(\ln(x)+b^2)^2}{2b^2}\right] dx \quad (15)$$

Equation (14) shows that  $P_e$  is large when either the links S-D and R-D are both in yawning fades or when the links S-D and S-R are both in deep fades thus reflecting the enhanced diversity order of the proposed cooperative system.

## VI. SIMULATION RESULTS

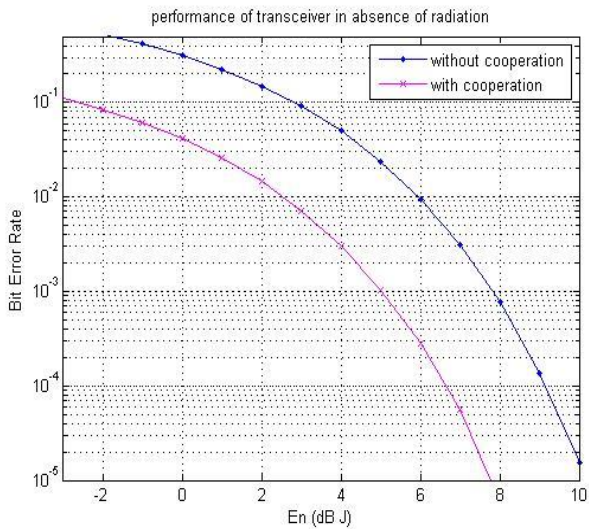


Fig 6.1: performance of transceiver in absence of radiation for Rayleigh fading channel

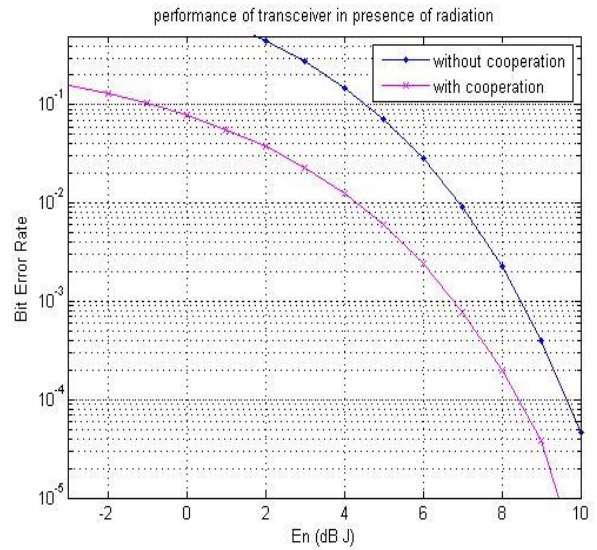


Fig 6.2: performance of transceiver in presence of radiation for Rayleigh fading channel

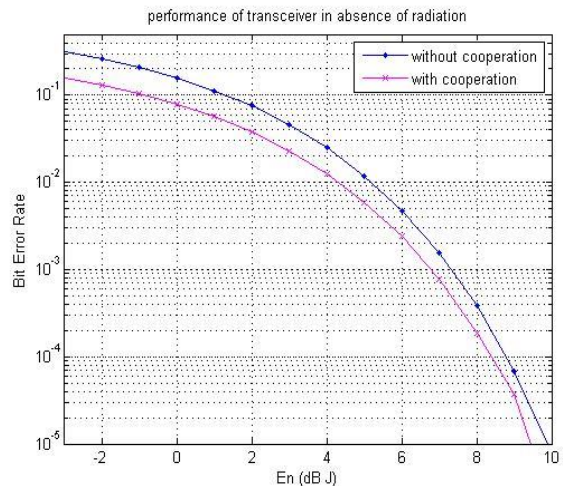


Fig 6.3: performance of transceiver in absence of radiation for lognormal fading channel

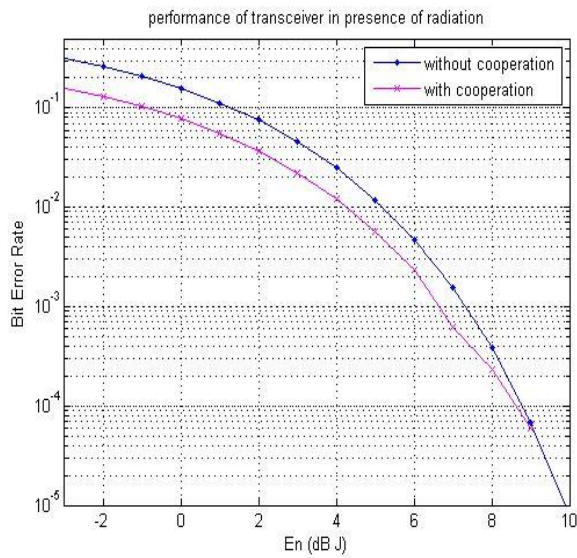


Figure 6.4: performance of transceiver in presence of radiation for lognormal fading channel

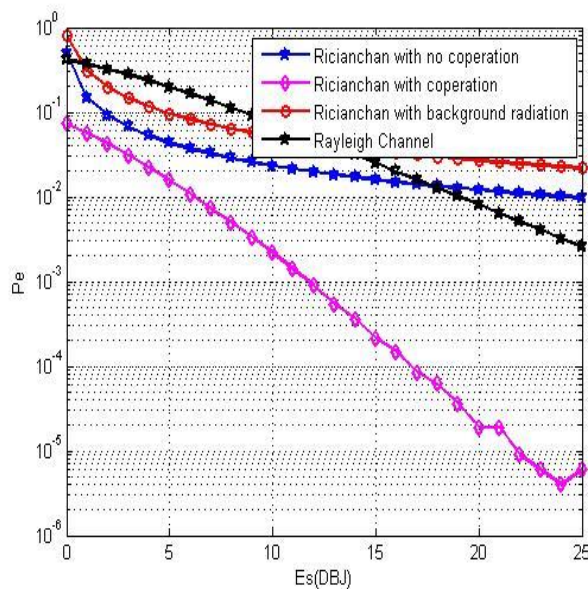


Fig. 6.5: Performance of 4-PPM for the Rician fading, Rayleigh case with background radiation.

This figure shows the excellent match between simulations and the exact SEP expression in eq. (14). The slopes of the SEP curves indicate that cooperation results in an increased diversity order of two for various distances of (R) from (S). Even in the extreme case where (S) is as far from (R) as it is from (D) ( $\beta = 1$ ), a gain of about 8 dB at a SEP of  $10^{-3}$  can be observed relative to non-cooperative systems.

The excellent match between simulations and eq.(12) can be seen in Fig 4 where a similar simulation setup is adopted in the case of lognormal fading with S.I. = 0.6. Results in Fig. 3 and Fig. 4 show that cooperation is

more beneficial in the case of Rician fading compared to lognormal fading where the performance gain can be realized at smaller error rates. This result is expected since the Rician distribution is used to model the scenario of severe fading while the lognormal model corresponds to the scenario of less severe fading. The superiority of the cooperative scheme over non-cooperative direct FSO links can be also seen in Fig. 4 in the presence of background radiation. As in the no-background radiation gains are more significant over Rician fading channels.

While the assumption of channel independence can be justified in MIMO wireless RF systems, there is a wide agreement that this assumption is not often valid in MIMO-FSO systems and, consequently, the high gains promised by MIMO techniques might not be realized in practice.

## VII.CONCLUSION

Despite the non-broadcast nature of FSO transmissions, this work showed that cooperative diversity can result in significant performance gains over the non-cooperative  $1 \times 1$  FSO links and over the  $2 \times 1$  MIMO-FSO links that suffer from correlated fading.

It was proven analytically that a full transmit diversity order can be achieved in the no-background radiation case. In the presence of background radiation, a numerical integration of the conditional SEP showed that the proposed scheme can maintain acceptable performance gains especially in the case of Rician fading. While this work analyzed cooperative diversity from a physical-layer point of view, future work must consider the implication of cooperation on higher layers.

## REFERENCES

- [1] D. Kedar and S. Arnon, "Urban optical wireless communications networks: the main challenges and possible solutions," *IEEE Commun. Mag.*, vol. 42, no. 5, pp. 2-7, Feb. 2003.
- [2] X. Zhu and J. Kahn, "Free-space optical communication through atmospheric turbulence channels," *IEEE Trans. Commun.*, vol. 50, no. 8, pp. 1293-1300, Aug. 2002.
- [3] M.-A. Khalighi, N. Schwartz, N. Aitamer, and S. Bourenane, "Fading reduction by aperture averaging and spatial diversity in optical wireless systems," *IEEE J. Optical Commun. Netw.*, vol. 1, pp. 580-593, Nov. 2009.
- [4] S. G. Wilson, M. Brandt-Pearce, Q. Cao, and J. H. Leveque, "Free-space optical MIMO transmission with Q-ary PPM," *IEEE Trans. Commun.*, vol. 53, pp. 1402-1412, Aug. 2005.
- [5] M. K. Simon and V. A. Vilnrotter, "Alamouti-type space-time coding for free-space optical communication with direct detection," *IEEE Trans. Wireless Commun.*, vol. 4, pp. 35-39, Jan. 2005.

- [6] S. Navidpour, M. Uysal, and M. Kavehrad, "BER performance of freespace optical transmission with spatial diversity," *IEEE Trans. Wireless Commun.*, vol. 6, no. 8, pp. 2813-2819, Aug. 2007.
- [7] T. Tsiftsis, H. Sandalidis, G. Karagiannidis, and M. Uysal, "Optical wireless links with spatial diversity over strong atmospheric turbulence channels," *IEEE Trans. Wireless Commun.*, vol. 8, no. 2, pp. 951-957, Feb. 2009.
- [8] J. Laneman and G. Wornell, "Distributed space time coded protocols for exploiting cooperative diversity in wireless networks," *IEEE Trans. Inf. Theory*, vol. 49, no. 10, pp. 2415-2425, Oct. 2003.
- [9] J. Laneman, D. Tse, and G. Wornell, "Cooperative diversity in wireless networks: efficient protocols and outage behavior," *IEEE Trans. Inf. Theory*, vol. 50, pp. 3062-3080, Dec. 2004.



Omkar naidu.v, PG Student, Dept of ECE, SITAMS, Chittoor. He received B.Tech degree from JNTU, Anantapur, doing his research work in wireless communication to receive M.Tech degree from JNTU, Anantapur, in communication systems. He presented various papers in national conferences.



K.M.Hemambaran, Assistant Professor, Dept of ECE, SITAMS, Chittoor. He had completed his M.Tech and Area of Interest in Digital and Communication. He presented and published in various national and international conferences and journals, and he is a life time member of IETE / ISTE.



T Kantharaju is currently working as an Assistant Professor in ECE department, BIT Institute of Technology, Hindupur. He has received Master of Engineering (M.E) degree from University Visvesvaraya College of Engineering Bangalore University, Bangalore.



Neerajakshi.V, PG Student, Dept of ECE, BIT institute of technology, Hindupur. She has received B.Tech degree from JNTU, Anantapur, doing his research work in wireless communication to receive M.Tech degree from JNTU, Anantapur. She presented various papers in national conferences.